Inorganic Chemistry

Article

pubs.acs.org/IC

Extended Ni(III) Oxyhalide Perovskite Derivatives: Sr_2NiO_3X (X = F, Cl)

Yoshihiro Tsujimoto,*[,†] Kazunari Yamaura,[‡] and Tetsuo Uchikoshi[†]

[†]Materials Processing Unit, National Institute for Materials Science, 1-2-1 Sengen, Tsukuba, Ibaraki 305-0047, Japan

[‡]Superconducting Materials Unit, National Institute for Materials Science, 1-1 Namiki, Tsukuba, Ibaraki 305-0044, Japan

ABSTRACT: Extended layered oxyhalide compounds, Sr_2NiO_3X (X = F, Cl), with the square pyramidal coordination around the trivalent nickel ions in the low spin state (S = 1/2), are successfully synthesized by a high-pressure and high-temperature reaction. Both these compounds crystallize in the n = 1 Ruddlesden−Popper type structure, but the difference of halogen anions incorporated dictate the anion-site ordering patterns and the magnetic ground states. Sr_2NiO_3F adopts the tetragonal cell in the space group $I4/mmm$ (a = b = 3.79125(2) Å and c = 13.13754(9) Å), with O/F anions being disordered at the apical sites, while the crystal structure of Sr_2NiO_3Cl is described in the tetragonal space group $P4/nmm$ (a = b = 3.85566(1) Å and c = 14.43240(6) Å) with O/Cl anions being fully ordered at the apical sites. Additionally, Sr_2NiO_3Cl undergoes a long-range antiferromagnetic order below T_N = 33 K, while the fluorine counterpart does not exhibit a long-range ordering but spin glass transition at T_{SG} = 11 K. In light of the positive Weiss temperatures for both X = F and Cl, the unpaired electron likely occupies a d(xy) orbital. Namely, the superexchange interaction mediated by d(xy)-Opπ-d(xy) in the NiO_2 basal plane is antiferromagnetic, while the direct exchange interaction between d(xy)-d(xy) along the diagonal directions is ferromagnetic. The origin of spin glass behavior observed in X = F is probably due to randomness of the direct d(xy)-d(xy) bonds caused by off-centering nickel ions and O/F site disordering.

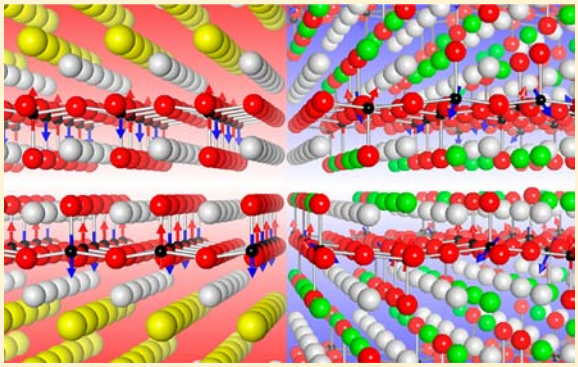

1. INTRODUCTION

Development of the understanding of the transition metal oxides has triggered the search for heteroanion containing metal oxides because incorporation of hetero anions which possess different charge, electronegativity, and ionic size from the oxide ion opens up possibilities for inducing new physical and chemical properties that the corresponding pure oxide does not exhibit.[1−4] Basically, the electronic states of d transition metals are controlled with mixed anions in two ways. One is tuning of the covalent interactions between the transition metal cations and the neighboring anions while keeping the coordination environment, which directly affects the band gap structure, the crystal field energy, and spin, charge, and orbital degrees of freedom of the cations. This is exemplified by the photocatalytic activity under visible light in oxynitrides,[1] and strong enhancement of the superexchange interaction mediated by hydride anions in oxyhydrides.[5] The other involves coordination rearrangement by partially substituting oxide ions by hetero anions weakly bound to the metal center, which is seen in layered oxyhalide and oxysulfide compounds. For example, $Sr_2CoO_2Cl_2$,[6] $Sr_3Co_2O_4Cl_2$,[7] $Sr_2Cu_2CoO_2S_2$[8] possess the c-axis elongated octahedron $CoO_4(Cl/S)_2$, but the coordination environment can be regarded as square planar geometry in light of the first coordination sphere. Indeed, their physical properties can be understood on the basis of the electronic configuration expected from square planar coordination.

The number of reports on extended transition metal compounds with mixed anions has been increasing recently. However, the variety of the transition metal center is substantially limited. One such element studied to a lesser extent is nickel. Ni-based layered perovskites belonging to Ruddlesden−Popper (RP) type structure expressed as $A_{n+1}Ni_nO_{3n+1}$ (A = alkali, alkaline earth, or rare earth metal) have been vastly investigated in terms of similarity to superconducting copper oxides. It is reported that $La_{2-x}Sr_xNiO_4$ exhibits a metal−insulator transition and static order of charge and spin in some x regime.[9−12] In addition, infinite NiO_2 planes resembling superconducting CuO_2 planes are formed by topotactic reductions in a homologous series of nickelates $A_{n+1}Ni_nO_{2n+2}$.[13,14] The nickel oxides show a rich variety of structural and physical properties by cation doping and oxide sublattice modification. On the other hand, there have been few studies focused on the effects of heteroanion doping into nickel oxide perovskites. The only example is a Dion−Jacobson type layered perovskite $(NiCl)Sr_2Ta_3O_{10}$[15] prepared by an ion-exchange reaction. In the structure the divalent nickel center is tetrahedrally coordinated by two apical oxide ions and two chloride ions in the equatorial positions between the perovskite block layers.

Herein, we report high-valent nickel oxyhalide perovskite derivatives, $Sr_2Ni^{3+}O_3X$ (X = F, Cl), isostructural with the RP

Received: August 4, 2013
Published: August 21, 2013

structure of n = 1. The new phases synthesized by a high-pressure and high-temperature technique are the first examples of incorporation of oxygen and halogen anions in trivalent centered perovskite compounds. The kind of halogen anion incorporated makes a big difference in the structure, anion ordered pattern, and magnetic properties. Sr_2NiO_3Cl adopts the tetragonal structure with space group $P4/nmm$ with chlorine being ordered at the apical sites and undergoes an antiferromagnetic ordering at 33 K. In contrast, Sr_2NiO_3F crystallizes in the body-centered tetragonal $I4/mmm$ with fluorine being disordered at the apical sites and exhibits no long-range magnetic order but a spin glass transition at 11 K.

2. EXPERIMENTAL SECTION

Synthesis. Sr_2NiO_3X (X = F, Cl) was prepared from a stoichiometric mixture of in-house synthesized SrO_2, SrX_2 (99.9, High Purity Chemical Ltd.), and Ni (99.9, Rare Metallic Ltd.). The mixture was thoroughly ground in an agate mortar in a Ar-filled glovebox and heated in a belt-type high-pressure apparatus at 6 GPa and 1773 K for X = F and at 3 GPa and 1573K for X = Cl, in a Pt capsule. Then, the sample was quenched to room temperature, and the pressure was slowly released. Both the resultant products were black.

Characterization. The products were assessed by synchrotron X-ray diffraction (XRD), the data of which were collected at room temperature using a one-dimensional X-ray detector[16] installed at BL15XU, NIMS beamline (SPring-8). The wavelength was λ = 0.65298 Å. The sample was contained in a glass capillary of diameter 0.1 mm. The data were recorded in 0.003 increments in a 2θ range of 10−50°. Structural refinement was conducted using the Rietveld method with the program RIETAN-FP.[17] The pseudo-Voigt function was used as a profile function. The weighting R index (R_{wp}), the Bragg R index (R_I), and goodness of fit (S) are defined as follows; $R_{wp} = [\Sigma_i w_i(y_{io} - y_{ic})^2/\Sigma_i w_i y_{io}^2]$ and $R_I = \Sigma_k |I_{ko} - I_k|/\Sigma_k I_{ko}$, where y_{io} and y_{ic} are the observed and calculated intensities, w_i is the weighting factor, and I_{ko} and I_k are the observed and calculated integrated intensities. $S = R_{wp}/R_{exp}$. $R_{exp} = [(N-P)/\Sigma_i w_i y_{io}^2]^{1/2}$, where N is the total number of y_{io} data when the background is refined, and P is the number of adjusted parameters. Magnetic measurements were performed using a superconducting quantum interference device (SQUID) magnetometer (Quantum Design, MPMS-XL).

3. RESULTS AND DISCUSSION

Structural Characterization. Figure 1a displays the SXRD data collected at room temperature from Sr_2NiO_3F. SXRD data of Sr_2NiO_3F could be readily indexed by a simple body-centered tetragonal system in the space group $I4/mmm$, which is common to RP structure. The cell parameters are $a = b$ = 3.79125(2) Å and c = 13.13754(9) Å. No evidence for O/F ordering was found, but the c axis as long as that for an isostructural oxyfluoride Sr_2CoO_3F[18] suggests preferential occupation of fluorine at the apical anion sites. In principle, it is not possible to distinguish oxygen from fluorine by diffraction methods. Nevertheless, we can presume that fluorine atoms occupy the apical sites rather than the equatorial sites, as shown in related oxyfluoride compounds.[19−21] Initial Rietveld refinements based on a simple n = 1 RP structure where O/F atoms are disordered at the apical sites readily converged well, but the atomic displacement parameter of nickel site, U_{iso}(Ni), remained somewhat large, about 1.51 Å^2. This problem was resolved by displacing the nickel atom from 2a site (0, 0, 0) to 4e site (0, 0, z), which gave a reasonable value of U_{iso}(Ni) = 0.11 Å^2. The fractional occupancy of all of the anion sites remained the unity value within errors, and thus was fixed during the refinements. Figures 2a and 3a and Table 1 show the so-determined crystal structure, local coordination environment

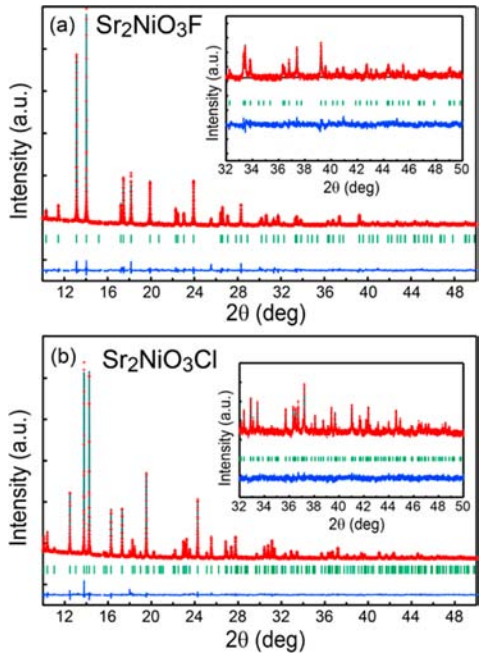

Figure 1. Observed (crosses), calculated (upper solid line), and difference (bottom solid line) plots from the Rietveld refinement against the SXRD data collected from (a) Sr_2NiO_3F and (b) Sr_2NiO_3Cl at room temperature. The inset is a magnified view in a high 2θ region.

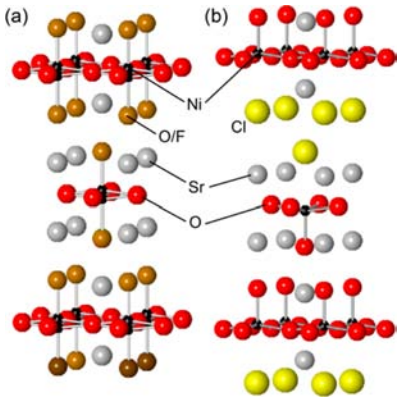

Figure 2. Crystal structures of (a) Sr_2NiO_3F and (b) Sr_2NiO_3Cl, with O and F/Cl anion sites being disordered/ordered at the apical sites. The Ni cation, which is off-centered because of the different bonding nature against oxygen and halogen, forms square pyramidal coordination with oxygen anions.

around the cations, and the crystallographic information of the oxyfluoride, respectively.

The SXRD patterns of Sr_2NiO_3Cl were also similar to those for the fluorine counterpart (Figure 1b). But closer inspection of the data revealed additional reflections indicative of symmetry lowering from $I4/mmm$ to $P4/nmm$, which is associated with O/Cl site ordering. Actually, a similar trend is commonly observed in related oxychloride compounds with O/Cl ordering at the apical sites, such as Sr_2BO_3Cl (B = Mn, Fe, Co).[22−24] The cell parameters are $a = b$ = 3.85566(1) Å and c = 14.43240(6) Å. Because of large ionic radius of chloride ion compared with fluoride ion, the c axis is significantly elongated while the a axis slightly increases. With a model based on the structure of Sr_2CoO_3Cl,[24] the crystal structure of Sr_2NiO_3Cl

dx.doi.org/10.1021/ic402008n | Inorg. Chem. 2013, 52, 10211−10216

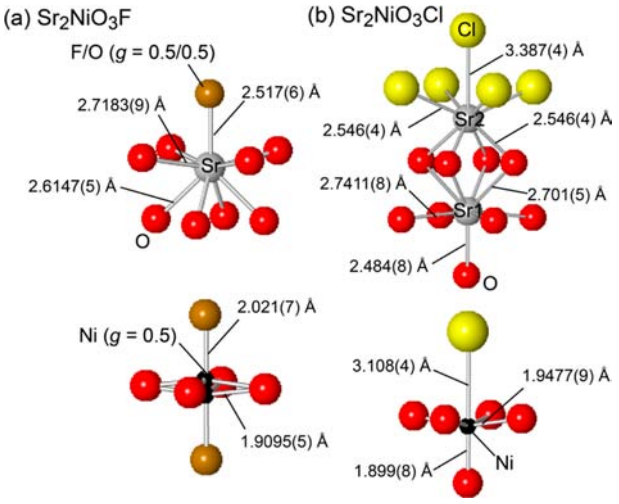

Figure 3. Local coordination environment around Ni and Sr centers for (a) Sr_2NiO_3F and (b) Sr_2NiO_3Cl.

Table 1. Crystallographic Parameters Refined from SXRD Data Collected from Sr_2NiO_3X (X = F, Cl) at Room Temperature[a]

atom	site	g[b]	x	y	z	B_{iso}/Å^2
Sr_2NiO_3F ($I4/mmm$: a = 3.79125(2) Å and c = 13.13754(9) Å)						
Sr	4*e*	1	0	0	0.36292(5)	0.494(14)
Ni	4*e*	0.5	0	0.5	0.0175(2)	0.11(4)
O_{eq}	4*c*	1	0	0	0	0.62(11)
O_{ap}/F	4*e*	0.5/0.5	0	0	0.1712(3)	2.19(9)[c]
Sr_2NiO_3Cl ($P4/nmm$: a = 3.85566(1) Å and c = 14.43240(6) Å)						
Sr1	2*c*	1	0.75	0.75	0.09590(6)	0.40(3)
Sr2	2*c*	1	0.75	0.75	0.34225(7)	0.48(2)
Ni	2*c*	1	0.25	0.25	0.2077(1)	0.08(3)
O_{eq}	4*f*	1	0.25	0.75	0.2269(3)	0.49(8)
O_{ap}	2*c*	1	0.25	0.25	0.0761(4)	0.91(12)
Cl	2*c*	1	0.25	0.25	0.4230(2)	0.93(6)

[a]The goodness of fit S and the R factors X = F and Cl are S = 2.17, R_{wp} = 1.64, and R_I = 6.09, and S = 1.65, R_{wp} = 1.41, and R_I = 6.21, respectively. [b]All site occupancies g were fixed to unity during the refinements. [c]B_{iso} values for O_{ap} and F are constrained to the same value.

was successfully refined. Refinements of the occupancy for all of the anion sites also revealed no anion vacancies within errors. The final refined structure and crystallographic data are given in Figures 2b, 3b, and Table 1, respectively.

To check the validity of the refined structures, we calculated the Bond-Valence-Sum (BVS)[25,26] for the metal cations in Sr_2NiO_3X (X = F, Cl). Since there is no reference of BVS parameters for Ni^{3+}−(F/Cl), the BVS parameter for Ni^{2+} was employed for bonds to halogen. As discussed below, this procedure does not cause a serious error for estimation of the BVS for Ni^{3+} in the present compounds because the bond length between the nickel cation and halogen anion is much longer than the sum of ionic radii of Ni^{3+} (0.56 Å) and F^-/Cl^- (1.33 Å /1.81 Å).[27] As for X = F, the BVS values of Ni and Sr are 3.10 and 2.04, respectively, consistent with those expected from the chemical formula. Additionally, the calculation of BVS for Ni and Sr2 in X = Cl resulted in 3.06 and 1.94, respectively, in good agreement with the expected values. The BVS for Sr1 is, however, 2.51, much larger than that expected from a simple ionic model. This result implies strong compression between Ni−O/Cl bonds.

The majority of coordinations around Ni^{3+} in nonmolecular solids is octahedral, as seen in $LaNiO_3$, $YbSr_3NiO_6$ and Na_3NiF_6.[28−30] The local coordination environment around the nickel center in this study is obviously different from the octahedral symmetry. The Ni atom moves away from the center position of the NiO_5X octahedron along the c direction, leading to a distorted square pyramidal coordination. To the best of our knowledge, this is the first example of square pyramidal coordination around trivalent nickel cation. The O_{eq}−Ni−O_{eq} bond angle on the basal plane is 166.2(3)° for X = F and 163.6(3)° for X = Cl, smaller than the ideal angle of 180°. Besides, the Ni−O_{ap} bond length is much shorter than that for the Ni−X bond; the ratio of Ni−O_{ap}/Ni−X is 0.815 (= 2.021 Å/2.480 Å) for X = F and 0.611 (= 1.899 Å/3.108 Å) for X = Cl. It is to be noted that the shorter and longer Ni−O_{ap}/F bonds are assumed as Ni−O_{ap} and Ni−F bonds, respectively, in light of the strong orbital hybridization between O and Ni atoms.

On the other hand, the halogen atom incorporated plays a crucial role in anion (dis)ordered patterns. In general, both the oxyfluoride and the oxychloride systems expressed as A_2BO_3X, O/X atoms exclusively occupy the apical sites in an ordered manner with the metal center being five-coordinated.[21] The O/F disordered state is exceptionally found in d^0 metal based compounds which take octahedral coordination.[31] In this sense, it is likely that the square pyramidal coordination leads to O/X site ordering. Another type of coordination environment was recently realized in the cobalt oxyfluoride Sr_2CoO_3F: the coexistence of O/F disordered state and square pyramidal coordination.[18] The nickel oxyfluoride in this study exactly follows this type of structural feature. Given that both Sr_2BO_3F (B = Co, Ni) are synthesized by a similar reaction method using a high pressure apparatus, the reaction conditions of pressure and/or temperature possibly causes anion disordering with the B cation five-coordinated. The reason for no O/Cl disordering is the big difference of ionic radius between chlorine and oxygen.

Magnetism. The present compounds with high-valent nickel ions also exhibit remarkable peculiarity in their magnetic properties. Figure 4 shows the temperature dependence of magnetic susceptibility ($\chi = M/H$) for Sr_2NiO_3X, measured at a magnetic field of 1 kOe under zero-field cooled (ZFC) and FC conditions. Both compounds exhibit smooth increase in the data with lowering temperatures, while following the Curie−Weiss law, $\chi = C/(T - \theta)$ in the range of 150 < T < 350 K where C and θ are the Curie constant and Weiss temperature, respectively. The fit to the data gave C = 0.488 (emu K)/mol and θ = 21.3 for X = F, and C = 0.421 (emu K)/mol and θ = 24.2 K for X = Cl. The C values for both oxyhalide compounds correspond to that expected from the low spin state of Ni^{3+} with S = 1/2, rather than the high spin state with S = 3/2. The positive Weiss temperatures, which have weak X dependence, indicate that ferromagnetic interaction is dominant.

On cooling down from 150 K, Sr_2NiO_3X exhibits the strong X dependence of magnetic properties. X = Cl shows no difference between ZFC and FC data and a broad maximum at 47 K, characteristic of low-dimensional antiferromagnets. Given the two-dimensional structure and magnetism in this phase, it is a good measure to assign the Néel temperature (T_N) from the temperature derivative of $\chi(T)$. Thus, T_N estimated from the temperature at which $d\chi(T)/dT$ reaches a maximum value is 33

dx.doi.org/10.1021/ic402008n | Inorg. Chem. 2013, 52, 10211−10216

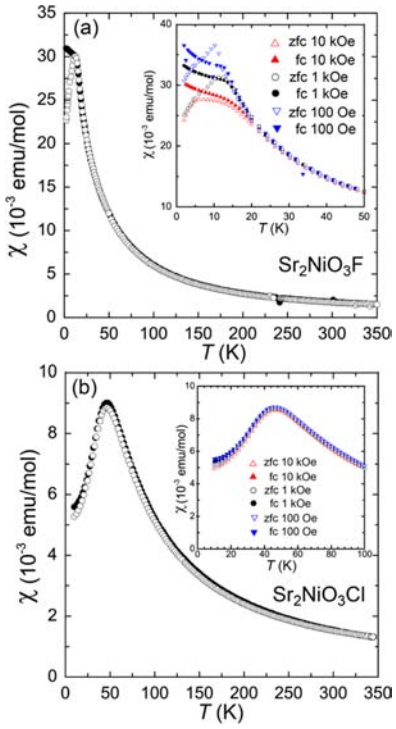

Figure 4. Temperature dependence of the magnetic susceptibility for (a) Sr_2NiO_3F and (b) Sr_2NiO_3Cl, measured under zero field cooled and field cooled conditions. The inset shows the field dependence of the magnetic susceptibility.

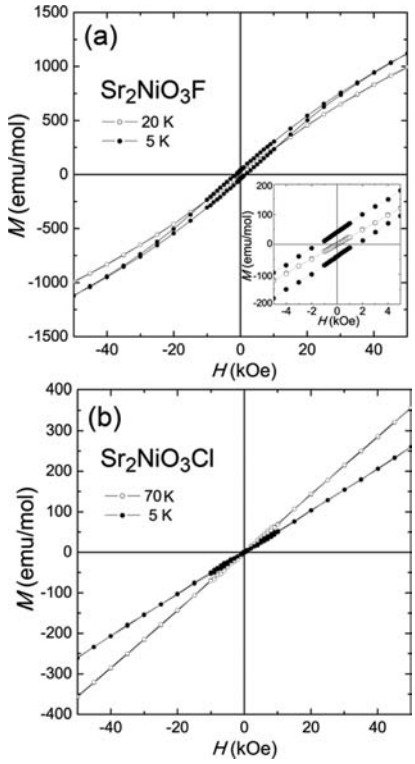

Figure 5. Isothermal magnetization curves of (a) Sr_2NiO_3F and (b) Sr_2NiO_3Cl measured at 5 and 20 or 70 K. The inset shows the data between −5 and 5 kOe.

K. In contrast, X = F revealed a divergence between ZFC and FC data below T_{SG} = 11 K in H = 1 kOe, suggesting a spin glass transition. As shown in the inset of Figure 4b, T_{SG} shifts to lower temperatures with increasing magnetic fields, followed by suppression of the divergence. Figure 5a shows the isothermal magnetization data for X = F where hysteresis loop was observed at 5 K ($<T_{SG}$), but not at 20 K ($>T_{SG}$). These behaviors are typically seen in spin glass materials.[32−35] Neither field dependence nor ZFC/FC divergence in the magnetization data appeared in the Cl counterpart (the inset in Figure 4b and Figure 5b).

Possible Electronic Configuration and Exchange Pathways. It is notable that Sr_2NiO_3X displays antiferromagnetically correlated phenomena in spite of the positive θ, and the drastic change in the magnetic ground state by F-to-Cl substitution. These features are never seen in the related oxyhalides such as Sr_2BO_3X (B = Mn, Fe, Co; X = F, Cl) with their large negative θ's,[19−21,36,37] but are reminiscent of the existence of strong competition or spin frustration between ferromagnetic (FM) and antiferromagnetic (AFM) interactions in the NiO_2 plane. The origin of FM interactions, however, is rather complex. As a simple electronic configuration for the low-spin Ni^{3+} with a square pyramidal geometry, we can presume $(xy)^2(xz,\ yz)^4(x^2-y^2)^1(3z^2-r^2)^0$ or $(xz,\ yz)^4(xy)^2(3z^2-r^2)^1(x^2-y^2)^0$. In both cases, superexchange couplings mediated by O_{2p} orbitals give rise to AFM interactions between the nearest neighbor (NN) nickel ions according to the Goodenough−Kanamori rule.[38] But, a FM superexchange pathway that dominates over the AFM interactions seems impossible. A plausible mechanism leading to dominant FM interactions is a specific orbital ordering induced by cooperative Jahn−Teller distortion, as observed in K_2CuF_4 with the n = 1 RP structure.[39] The Jahn−Teller active Cu^{2+} ions exhibit cooperative ordering of $d(z^2-y^2)/d(z^2-x^2)$ orbitals with the axes of [100] and [010] in CuF_2 plane, resulting in the ferromagnetic transition at T_c = 6.25 K. However, this is not true for our situation because conversely this type of orbital ordering does not allow for sizable AFM interaction. Here, we propose the electronic configuration compatible with the coexistence of AFM and FM interactions: $(xz,\ yz)^4(3z^2-r^2)^2(xy)^1(x^2-y^2)^0$. This configuration with an unpaired electron occupying an xz orbital is realized in an organometallic molecule where the trivalent nickel ion is surrounded by a square pyramid with one nitrogen atom in the apical site and two nitrogen and oxygen atoms in the basal plane.[40] In this case, we can expect that the $d(xy)$-$p\pi$ bond along the side directions of a NiO_2 square gives rise to AFM interaction between the NN nickel ions (J_1) while the direct exchange interaction through a $d(xy)-d(xy)$ bond along the diagonal ones (J_2) possibly leads to FM interaction (Figure 6). Basically, the shorter the bond the stronger the exchange interaction is. J_1, however, can have weaker interaction than J_2, owing to a small overlap associated with $\pi-\pi$ bonding and the corrugated basal plane.

Next, on the basis of our proposed J_1-J_2 model described above, we will discuss the question of what plays a critical role in determining the magnetic ground state, especially, the spin glass transition observed in Sr_2NiO_3F. It is well-known that spin glassy behavior results from spin frustration and/or bond randomness. For example, isostructural compounds such as $Rb_2Cu_{1-x}Co_xF_4$[41] and $La_{1-x}Sr_xBO_4$ (B = Mn, Co)[35,42] undergo spin glass transition because of the competition between FM and AFM J_1, which were induced by doping iso- or aliovalent metal cations. In contrast, Sr_2NiO_3F as well as Sr_2NiO_3Cl has no competion between AF and FM interactions in the NiO_2

dx.doi.org/10.1021/ic402008n | Inorg. Chem. 2013, 52, 10211−10216

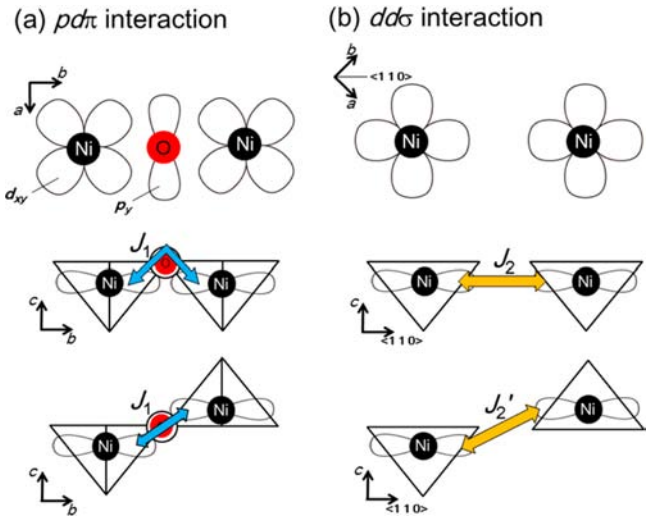

Figure 6. Relationship between orbital symmetry and exchange interactions in the NiO_2 plane. In contrast to J_1, J_2 depends on the O/*X* ordering patterns.

planes regardless of ordering patterns of *X* sites on the assumption of our model (see Figure 6). However, the anion disordering accompanied by off-centering of Ni ions from the basal plane in Sr_2NiO_3F makes the magnitude of the orbital hybridization inhomogeneous between the second NN nickel ions; d(*xy*) orbitals along the diagonal directions on the same plane with (0, 0, *z*) have larger overlap, while smaller overlap on the different planes, (0, 0, ± *z*). It is likely that this kind of bond mixing randomness of two kinds of FM J_2 results in a spin glass transition instead of a long ranged magnetic order. Indeed, Sr_2NiO_3Cl without such bond randomness undergoes a magnetic ordering. To investigate the validity of our proposed model, theoretical calculations or neutron experiments should be performed.

4. CONCLUSION

We have successfully synthesized new nickel oxyhalide compounds, Sr_2NiO_3X (*X* = F, Cl), which crystallize in the *n* = 1 RP structure while the *X* anion is ordered for Cl and disordered for F at the apical sites with the O anion. Both compounds take the square pyramidal coordination of Ni^{3+} leading to the low-spin state with *S* = 1/2. The O/*X* anion ordering is correlated with the magnetic ground states, which likely originates from bond randomness of FM interactions between d(*xy*) orbitals along the diagonal directions on a square. Theoretical calculation and/or syntheses of new members with similar electronic configuration (e.g., Ti^{3+} and V^{4+}) in the future will provide deeper insight into the mechanism of the unusual electronic and magnetic states for the present nickel oxyhalides.

AUTHOR INFORMATION

Corresponding Author

*E-mail: TSUJIMOTO.Yoshihiro@nims.go.jp.

Author Contributions

The manuscript was written through contributions of all authors.

Notes

The authors declare no competing financial interest.

ACKNOWLEDGMENTS

We thank H. Manaka, K. Miyano, and R. Tamura for helpful discussions, Y. Katsuya, M. Tanaka, and O. Sakata for supporting the SXRD experiments (2013A4504), and M. Miyakawa, K. Fujimaki, and T. Taniguchi for support with the high-pressure synthesis at NIMS. This work was supported by a Grant-in-Aid for Research Activity (25289233, 22246083) and a Funding Program for World-Leading Innovative R&D on Science and Technology (FIRST) from JSPS, and the Advanced Low Carbon Technology Research and Development Program (ALCA) of JST.

REFERENCES

(1) Ishikawa, A.; Takata, T.; Kondo, J. N.; Hara, M.; Kobayashi, H.; Domen, K. *J. Am. Chem. Soc.* **2002**, *124*, 13547−13553.
(2) Kobayashi, Y.; Hernandez, O. J.; Sakaguchi, T.; Yajima, T.; Roisnel, T.; Tsujimoto, Y.; Morita, M.; Noda, Y.; Mogami, Y.; Kitada, A.; Ohkura, M.; Hosokawa, S.; Li, Z.; Hayashi, K.; Kusano, Y.; Kim, J.; Tsuji, N.; Fujiwara, A.; Matsushita, Y.; Yoshimura, K.; Takegoshi, K.; Inoue, M.; Takano, M.; Kageyama, H. *Nat. Mater.* **2012**, *11*, 507−511.
(3) Al-Mamouri, M.; Edwards, P. P.; Greaves, C.; Slaski, M. *Nature* **1994**, *369*, 382−384.
(4) Hiroi, Z.; Kobayashi, N.; Takano, M. *Nature* **1994**, *371*, 139−141.
(5) Hayward, M. A.; Cussen, E. J.; Claridge, J. B.; Bieringer, M.; Rosseinsky, M. J.; Kiely, C. J.; Blundell, S. J.; Marshall, I. M.; Pratt, F. L. *Science* **2002**, *295*, 1882−1884.
(6) Knee, C. S.; Weller, M. T. *J. Solid State Chem.* **2002**, *168*, 1−4. Knee, C. S.; Weller, M. T. *Phys. Rev. B* **2004**, *70*, 144406−144413.
(7) Romero, F. D.; Coyle, L.; Hayward, M. A. *J. Am. Chem. Soc.* **2012**, *134*, 15946−15952.
(8) Zhu, W. J.; Hor, P. H.; Jacobson, A. J.; Crisci, G.; Albright, T. A.; Wang, S.-H.; Vogt, T. *J. Am. Chem. Soc.* **1997**, *119*, 12398−12399.
(9) Takeda, Y.; Kanno, R.; Sakano, M.; Yamamoto, O.; Takano, M.; Bando, Y.; Akinaga, H.; Takita, K.; Goodenough, J. B. *Mater. Res. Bull.* **1990**, *25*, 293−306.
(10) Chen, C. H.; Cheong, S.-W.; Cooper, A. S. *Phys. Rev. Lett.* **1993**, *71*, 2461−2464.
(11) Cheong, S.-W.; Hwang, H. Y.; Chen, C. H.; Batlogg, B.; Rupp, L. W., Jr.; Carter, S. A. *Phys. Rev. B* **1994**, *49*, 7088−7091.
(12) Schilling, A.; Dell'Amore, R.; Karpinski, J.; Bukowski, Z.; Medarde, M.; Pomjakushina, E.; Müller, K. A. *J. Phys.: Condens. Matter* **2009**, *21*, 015701−015707.
(13) Lacorre, P. *J. Solid State Chem.* **1992**, *97*, 495−500.
(14) Poltavets, V. V.; Lokshin, K. A.; Dikmen, S.; Croft, M.; Egami, T.; Greenblatt, M. *J. Am. Chem. Soc.* **2006**, *128*, 9050−9051.
(15) Tsujimoto; Kitada, A.; Uemura, Y. J.; Goko, T.; Aczel, A. A.; Williams, T. J.; Luke, G. M.; Narumi, Y.; Kindo, K.; Nishi, M.; Ajiro, Y.; Yoshimura, K.; Kageyama, H. *Chem. Mater.* **2010**, *22*, 4625−4631.
(16) Tanaka, M.; Katsuya, Y.; Matsushita, Y.; Sakata, O. *J. Ceram. Soc. Jpn* **2013**, *121*, 287−290.
(17) Izumi, F.; Momma, K. *Solid State Phenom.* **2007**, *130*, 15−20.
(18) Tsujimoto, Y.; Li, J. J.; Yamaura, K.; Matsushita, Y.; Katsuya, Y.; Tanaka, M.; Shirako, Y.; Akaogi, M.; Takayama-Muromachi, E. *Chem. Commun.* **2011**, *47*, 3263−3265.
(19) Needs, R. L.; Weller, M. T.; Scheler, U.; Harris, R. K. *J. Mater. Chem.* **1996**, *6*, 1219−1224.
(20) Simon Case, G.; Hector, A. L.; Levason, W.; Needs, R. L.; Thomas, M. F.; Weller, M. T. *J. Mater. Chem.* **1999**, *9*, 2821−2827.
(21) Tsujimoto, Y.; Yamaura, K.; Takayama-Muromachi, E. *Appl. Sci.* **2012**, *2*, 206−219.
(22) Hector, A. L.; Hutchings, J. A.; Needs, R. L.; Thomas, M. F.; Weller, M. T. *J. Mater. Chem.* **2011**, *11*, 527−532.
(23) Knee, C. S.; Weller, M. T. *Chem. Commun.* **2002**, 256−257.
(24) McGlothlin, N.; Ho, D.; Cava, R. J. *Mater. Res. Soc.* **2000**, *35*, 1035−1043. Loureiro, S. M.; Felser, C.; Huang, Q.; Cava, R. J. *Chem. Mater.* **2000**, *12*, 3181−3185.

(25) Brown, I. D.; Altermatt, D. *Acta Crystallogr.* **1985**, *B41*, 244−247.
(26) Brese, N. E.; O'Keeffe, M. *Acta Crystallogr.* **1991**, *B47*, 192−197.
(27) Shannon, R. D. *Acta Crystallogr.* **1976**, *A32*, 751−767.
(28) García-Muñoz, J. L.; Rodríguez-Carvajal, J.; Lacorre, P.; Torrance, J. B. *Phys. Rev. B* **1992**, *46*, 4414−4425.
(29) James, M.; Attfield, J. P. *J. Mater. Chem.* **1994**, *4*, 575−578.
(30) Henkel, V. H.; Hoppe, R. *Z. Anorg. Allg. Chem.* **1969**, *364*, 253−262.
(31) Needs, R. L.; Weller, M. T.; Scheler, U.; Harris, R. K. *J. Mater. Chem.* **1996**, *6*, 1219−1224.
(32) Niu, H.; Fukushima, N.; Ando, K. *Phys. Rev. B* **1999**, *44*, 4724−4726.
(33) Wiebe, C. R.; Greedan, J. E.; Kyriakou, P. P.; Luke, G. M.; Gardner, J. S.; Fukaya, A.; Gat-Malureanu, I. M.; Russo, P. L.; Savici, A. T.; Uemura, Y. J. *Phys. Rev. B* **2003**, *68*, 134410−1−10.
(34) Belik, A. A.; Matsushita, Y.; Tanaka, M.; Takayama-Muromachi, E. *Angew. Chem., Int. Ed.* **2010**, *49*, 7723−7727.
(35) Moritomo, Y.; Higashi, K.; Matsuda, K.; Nakamura. *Phys. Rev. B* **1997**, *55*, R14725−14728.
(36) Menil, F.; Kinomura, N.; Fournes, L.; Portier, J.; Hagenmuller. *Phys. Status Solidi* **1981**, *64*, 261−274.
(37) Tsujimoto, Y.; Sathish, C. I.; Hong, K.-P.; Oka, K.; Azuma, M.; Guo, Y.; Matsushita, Y.; Yamaura, K.; Takayama-Muromachi, E. *Inorg. Chem.* **2012**, *51*, 4802−4809.
(38) Goodenough, J. B. In *Magnetism and the Chemical Bond*; Cotton, F. A., Olah, G. A., Prigogine, I., Eds.; Interscience monographs Chemistry; John Wiley & Sons: New York, 1963; Vol. *1*, pp 165−184.
(39) Khomskii, D. I.; Kugel, K. I. *Solid State Commun.* **1973**, *13*, 763−766.
(40) Hikichi, S.; Yoshizawa, M.; Sasakura, Y.; Komatsuzaki, H.; Morooka, Y.; Akita, M. *Chem.—Eur. J.* **2011**, *7*, 5011−5028.
(41) Dekker, C.; Arts, A. F.; de Wijn, H. W. *Phys. Rev. B* **1988**, *38*, 11512−11522.
(42) Moritomo, Y.; Tomioka, Y.; Asamitsu, A.; Tokura, Y.; Matsui, Y. *Phys. Rev. B* **1995**, *51*, 3297−3300.